

A case study of lightning coupling simulations supporting the design of new aircraft

José Antônio de Souza Mariano^{1,2}, Antônio Carlos da Cunha Migliano^{2,3}, Rodrigo Cabaleiro Cortizo Freire¹

1 - Chief Engineer Office - EMBRAER

2 - Instituto Tecnológico de Aeronáutica

3 - Instituto de Estudos Avançados

São José dos Campos - SP, Brasil.

jose.mariano@embraer.com.br, accmigliano@gmail.com, rodrigo.freire@embraer.com.br

Abstract — This paper presents an application of computational electromagnetics (CEM) and low level injection techniques to determine the electrical transients that may appear in an aircraft wiring during a lightning strike. The study was accomplished in four steps: first, the main electromagnetic coupling mechanisms to a specific sensor interface and its interconnecting cables were identified and characterized in the test bench; then an electromagnetic model was developed to support the understanding of the coupling problem. The knowledge attained from this experiment was further applied to develop a realistic numerical model intended to represent the aircraft installation and its predictions were validated against the actual transient levels obtained from the full aircraft test. As the final step, a design modification was proposed and evaluated.

Keywords— Computational Electromagnetics, EMC, Lightning Strikes, Aircraft Safety, Numerical Modeling, CEM

I. INTRODUCTION

Modern aircraft are designed to withstand the severe lightning environment defined by current airworthiness regulations [1]. Compliance with such strict standards has ensured the safety of commercial flight service in the recent history of aviation. To achieve robust and reliable system operation, aircraft manufacturers usually devise their development process from the concept stage to the final product assembly by taking into account proper system architecture, redundancy and segregation of critical functions, design goals oriented towards electromagnetic compatibility and a fair amount of bench and platform verification tests augmented by analysis [2], [3] and [4].

Nonetheless, the increasing reliance on electronics to perform critical control and navigation functions as well as the application of composite materials in the manufacturing of primary structural parts has placed a burden on the traditional means of achieving a complete design verification, not just for lightning indirect effects, but for many other aspects of electromagnetic compatibility [5]. In this context, computational electromagnetics (CEM) offers an interesting prospect: it can be perfected to limit the amount of verification tests on the actual installation, thus preventing the exponential growth of test matrices. It also allows tradeoff studies to be performed earlier in the development phase aiding a more

complete evaluation of attach-detach scenarios unfeasible to accomplish otherwise.

Moreover, the aircraft industry has taken advantage of analytical techniques such as numerical modeling to support product development, regarding the interaction and the effects of lightning, in a variety of engineering studies, for example:

- a) To determine aircraft zones where the leader inception is most likely to occur;
- b) To estimate lightning current distribution in complex structures and determine bench test levels for direct effects evaluation;
- c) To evaluate the possibility and extension of damages in composite parts;
- d) To determine induced transients in hydraulic tubing.

This paper discusses a practical application of CEM to evaluate the effects of a design change in an air data speed sensor of a commercial regional jet concerning the indirect effects of a lightning attachment to the sensor structure. The work was completed in four steps: first, the main coupling mechanisms were investigated and characterized in the laboratory with the aid of a metallic test box; a simple model was developed to represent this experiment. The parameters from this simpler study were used to develop a complete model of the aircraft nose section in order to simulate the electromagnetic coupling to the sensor wiring in a realistic manner. Once this validation step was achieved, the aircraft model was used to predict the effects of the degradation of the transfer impedance that exists between the sensor plate and the fuselage. The deterioration of the contact quality is due to a modification of the electrical bonding concept, which translates into overall higher design quality throughout the product life cycle in respect to maintenance.

II. METHODOLOGY

Design verification of aircraft systems against electromagnetic threats relies on the statistical characterization of the physical phenomena, definition of the idealized external environment, which preserves the parameters related to damaging and functional upsets of electronic circuits and a combination of many techniques to determine the internal

coupling to critical equipment interfaces [1]. Some of these techniques, which have been applied in this study, are described in the following sections.

A. Identification of the main coupling mechanisms

Typical transient waveforms measured at aircraft wiring often result from a combination of the following physical mechanisms [2]:

- Resistive coupling (e.g. Voltage rise due to the current flowing through the electrical resistance of ground planes and structural joints);
- Current diffusion through low conductive materials;
- Current redistribution due to shape and size of the structure;
- Magnetic flux leakage through apertures and seams;
- Structural and/or cable resonances due to the interaction between the capacitive and the inductive coupling;

A numerical simulation of a direct lightning attachment to the sensor metallic case (see Fig. 1) suggests that the current transfer function of all cables running under the cockpit floor all the way down to the forward electronic bay should not be, to a great extent, dominated by inductive coupling through the cockpit main apertures.

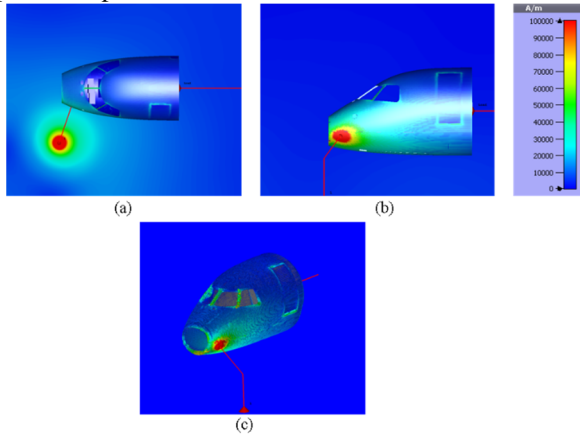


Fig. 1. (a) and (b) are different views of magnetic field distribution at 6.4 μ s in A/m. (c) Surface current distribution at 6.4 μ s in A/m.

Fig. 2 shows the color plot of the electric and magnetic field spatial distribution at the moment when the injected current reaches its maximum. The high intensity fields coupled through the cockpit main apertures, rapidly decay by the inverse of the distance and are effectively attenuated near the sensor cabling. Moreover, the complete harness topology from the sensor connector to the electronic modular unit is routed inside a metallic fuselage and is 2.7 meters long, which decreases resistive coupling due to the current flow through the metallic fuselage cross section and its structural joints to a negligible level. Therefore, the main energy-coupling path for this attachment scenario is through the transfer resistance of the sensor plate-fuselage joint. A faithful representation of this region is of paramount importance to be able to predict the coupling to the interconnecting cables within acceptable margins.

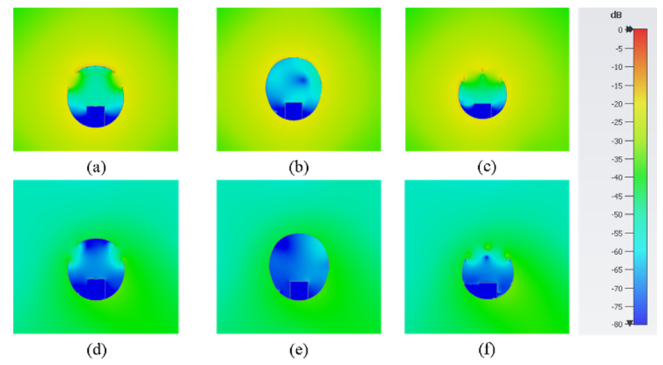


Fig. 2. 2D plots of electric field leakage at 6.4 μ s in dB. (a), (b), (c). 2D plots of magnetic field leakage at 6.4 μ s in dB. (d), (e), (f). The three cutting planes show the field coupling through the lateral windows, door slit and frontal widows respectively.

B. Laboratory tests on the metallic box

The development of a high fidelity electromagnetic model of a specific installation inside the aircraft fuselage depends on the effective identification and correct characterization of the main electromagnetic coupling mechanisms as well as on the accurate mapping of the lightning current paths through the structure.

Fig. 3, shows the test setup used to characterize the transfer impedance of the sensor mounting in the test bench. In this configuration, the lightning pulse generator is calibrated to achieve a scaled 1.0 kA component A according to the current wave shape defined by Eq 1.0 and graphed in Fig. 4. Parameters such as peak current, rate of rise to peak and action integral are derived from the statistical data available, for both negative cloud to ground and positive ground to cloud flashes considering a probability of exceedance of 5% [1]. The frequency content of component A is shown in Fig. 5. The generator is directly attached to the pitot tube and is grounded at the bottom of the box. Pin and bundle currents were recorded during the test. There are two separate connectors on the sensor case: one for the 10 AWG power cables and one for the sensing signals which is comprised of six 24 AWG twisted shielded pairs, one twisted shielded triple and one 22 AWG single wire bundled together inside a 7.5 mm braided shield. The selected pins for validation are presented in Table I. The dimensions of the test box is 1m×1m×0.5m with 2.0 mm average thickness. The sensor is mounted on the removable plate according to installation requirements such as surface cleanup and torque specifications.

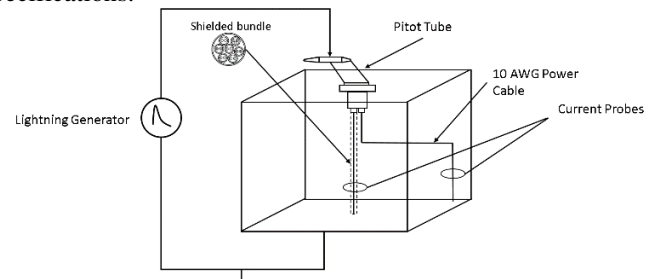


Fig. 3. Test setup for model development and parameter characterization

TABLE I: SELECTED PINS FOR VALIDATION

PIN	01	11	PIN 35	PIN E
Wire Type	S*	TSP**	TSP	S
Wire Gauge (AWG)	22	24	24	10
* Unshielded single wire				
** Twisted shielded pair				

When the lightning current flows through the contact resistance of the fuselage/sensor interface, neglecting nonlinear effects, there is a voltage rise through the transfer resistance of this joint, which can be understood as a forcing voltage function on the external loop that exists between the bundle shield and the metallic walls of the test box. The time constants of the current over the inner shielded cables are somewhat determined by the inductance and DC resistance of this loop as well as by the transfer resistance of the joint. This external loop current diffuses through the transfer impedance of the outermost shield and drives the internal currents that flow through the individual cable shields grounded, by design choice, at both ends. Likewise, the pin voltages are driven by the flow of this very current through the transfer impedance of individual cable shields. The developed common mode voltage (Voc) can also be interpreted as a forcing voltage function that will drive the pin short circuit current (Isc) through the inner impedance of the twisted shielded pairs once both sides of the same wire are shorted to the ground.

$$i(t) = I_0(e^{-\alpha t} - e^{-\beta t})(1 - e^{-\gamma t})^2 \quad (1)$$

$$I_0 = 218.810$$

$$\alpha = 11.354 \text{ s}^{-1}$$

$$\beta = 647.265 \text{ s}^{-1}$$

$$\gamma = 5.423.540 \text{ s}^{-1}$$

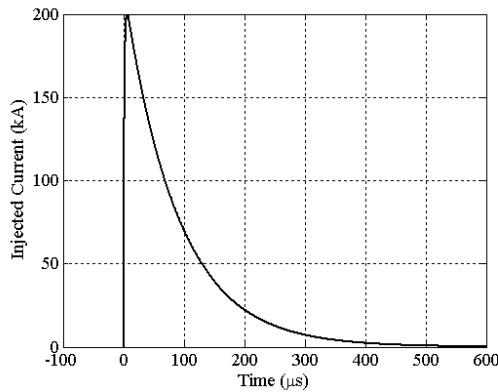


Fig. 4. Lightning component A [1]

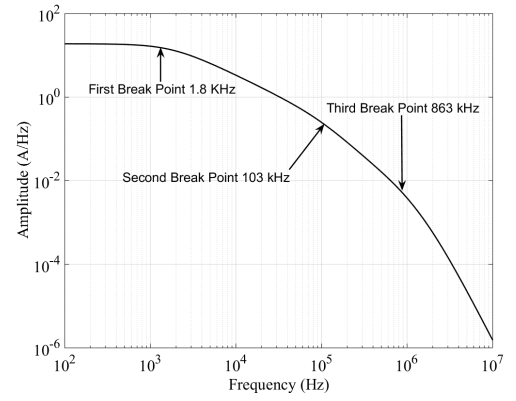


Fig. 5. Frequency content of component A [1]

Although the voltage rise across metallic joints is seldom a problem in itself, regarding indirect effects of lightning, high currents may transfer to the related wiring due to the low impedance paths provided by short cable shields. In fact, the measured voltages inside the test box and in the aircraft wiring were very close to noise floor and therefore most of the readings were overshadowed by the high frequency noise from the generator arc. The maximum predicted value, considering the injection of 1.0 kA, is 0.1 V.

C. Full aircraft tests

Full aircraft tests are aimed at determining the actual transient levels (ATL's) at critical equipment interfaces during a severe lightning event. The first return stroke represents the most significant electrical stress and therefore poses the greatest threat for systems. To verify protection against this environment it is common practice to measure the open circuit voltage and short circuit current in order to define the Thévenin equivalent circuit seen from the equipment interface during a lightning strike [4]. Equipment are then tested at the laboratory with scaled high levels derived from the aircraft verification tests and incorporating enough margins to account for uncertainties in the process (usually referred to as equipment transient design levels or ETDL's). In addition, onboard critical systems are designed to withstand the effects of short-pulse randomly distributed subsequent strokes that flow through the low impedance ionized path formed during the process of dielectric breakdown of air. Subsequent strokes usually do not represent a threat of damaging the interfaces but their steep time variation may drive functional upsets. To verify that the design is robust enough to prevent this situation from happening, aircraft systems undergo cable bundle tests (calibrated current injection over harnesses) that simulate the expected transients due to both cloud-to-earth and cloud-to-cloud lightning strikes [3].

SAE ARP 5416 outlines the low-level injection techniques most suitable for verification of new aircraft designs [4]. The test method applied in this work consists of adequately placing a coaxial return array around the aircraft to distribute the driving current and the related magnetic field evenly around the

fuselage thus matching the inflight condition as exemplified in Fig. 5. The cable currents and voltages were measured at selected interfaces to derive transient levels for equipment qualification tests.

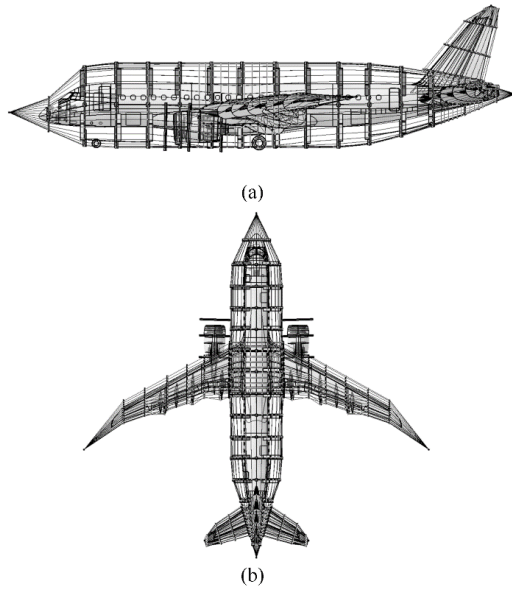


Fig. 6. Coaxial return array designed for a low level injection test on the aircraft. (a) Side view. (b) Top view.

D. Development of the aircraft numerical model

Once the validation of the test box was achieved, the related parameters were transferred to a representative model of the aircraft cockpit area. The aircraft model is cropped according to proper simplification assumptions to allow for reasonable computation times [6], [7].

Because the lightning pulse considered for design purposes, has a broad frequency spectrum it is expected that different frequency components will excite different electromagnetic phenomena. Concerning the current flow through the structure, the higher frequency components will tend to flow through the path of least inductance, while the lower frequency content will follow the path of least resistance. The geometric part of the problem is resolved by importing high fidelity cad models directly from the product structure. The material characteristics are assigned according to datasheet specifications and/or bonding measurements and each cad part is modeled taking into account the mean cross section so that the bulk resistance is adequately represented.

Fig. 6 shows the actual cable routing from the signal connector to the modular electronic unit where the data processing takes place and from the power connector to the power distribution bus located at the forward electronic bay. The harness model takes into account the existence of intermediate points of electrical bonding, the measured transfer impedance of braided shields and wire gauge from design specifications.

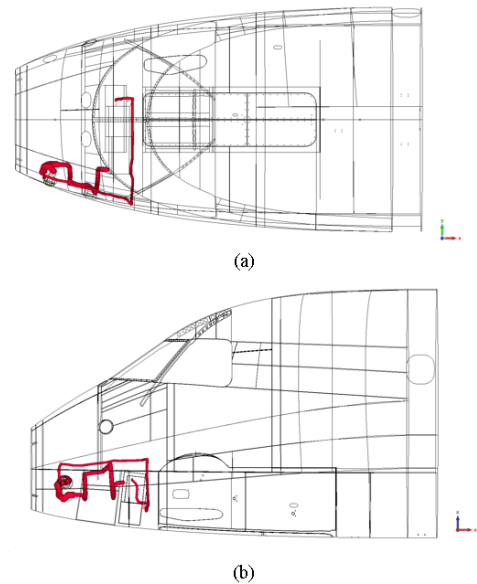


Fig. 7. Topology of the actual installed harness. a) Upper view. b) side view.

When performing time domain simulations, it is useful to sample the fields in time to ensure that the physics are correctly represented. These visual cues, as shown in Fig. 8 for example, are also helpful to establish a better understanding of the coupling paths and the model features where local mesh treatments are necessary for an accurate solution. Some of the physical aspects that are expected on simulations of lightning attachment to aircraft are:

- Skewed surface current distribution due to the attach-detach configuration;
- Negligible reflections at the boundaries matching the effects of a balanced return array or the expected inflight condition;
- Field enhancement around discontinuities;
- Leakage through apertures, seams and slots;
- Diffusion through composite parts at later times;
- Current flow through carbon parts at early times;
- Redistribution from carbon to metal parts at later time steps.

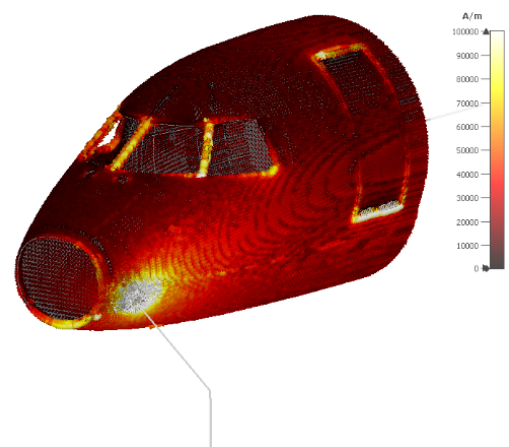


Fig. 8. Surface current density at 6.4

III. RESULTS

The main results obtained from the first experiment are summarized in Table II. Both the box and aircraft numerical models were simulated with a 25 mm spatial resolution and frequency bandwidth of 25 MHz using the TLM method implemented in the CST Studio Suite™ 2017. A 25mm×25mm seam was implicitly modeled with $3.8 \times 10^4 \Omega.m$ to represent the critical joint between the sensor plate and the fuselage at the baseline assembly. This configuration includes a polyurethane gasket with an embedded copper mesh that improves the transfer resistance between the sensor plate and the fuselage. Comparisons of bulk and pin currents are presented in Fig. 7, Fig. 8 and Fig. 9.

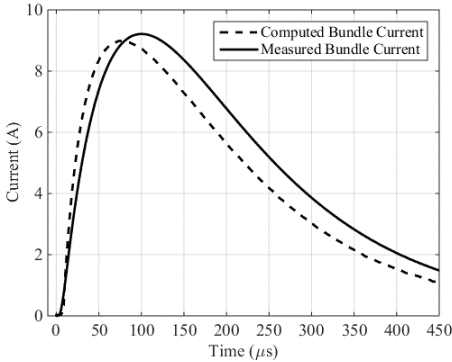


Fig. 9. Bulk cable current over the bundle shield for the baseline configuration of the test box

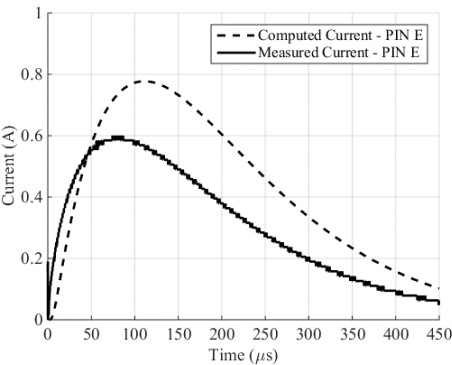


Fig. 10. Pin current on a 10 AWG wire on the baseline configuration of the test box

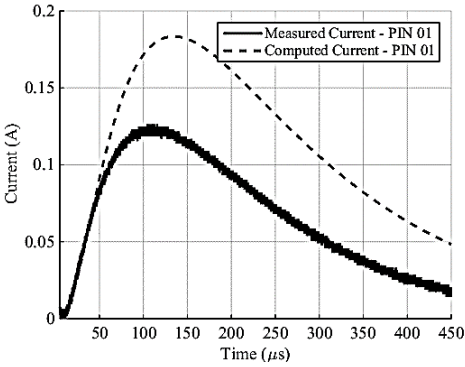


Fig. 11. Pin current on a 22 AWG wire on the baseline configuration of the test box

TABLE II: SUMMARY OF RESULTS – SHORT CIRCUIT CURRENT IN AMPERE FOR BASELINE CONFIGURATION

Method	Cable Bundle	PIN 01	PIN 11	PIN 35	PIN E
Measurement	8.98	0.17	0.13	0.15	0.60
Calculation	9.17	0.30	0.19	0.20	0.77

The results for the modified configuration are presented in Table III. By removing the conductive gasket the transfer resistance of the joint increases. To reflect this modification in the aircraft model, the conductivity of the joint was adjusted to $2.3 \times 10^4 \Omega.m$.

TABLE III: SUMMARY OF RESULTS – SHORT CIRCUIT CURRENT IN AMPERE FOR MODIFIED CONFIGURATION

Method	Cable Bundle	PIN 01	PIN 11	PIN 35	PIN E
Measurement	16.00	0.35	0.25	0.25	1.00
Calculation	14.80	0.48	0.29	0.63	1.19

Both the laboratory and aircraft predicted peak values agree with measurements within 1.58 dB. Furthermore, a qualitative inspection of the wave shapes (Fig. 11 to Fig. 13) indicates a fair agreement between the computed and measured currents in the aircraft wiring as well. These comparisons can be further considered to evaluate the accuracy of both verification methods and develop appropriate margins to account for analysis and test uncertainties.

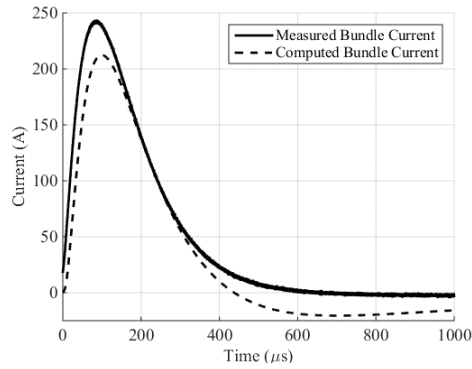


Fig. 12. Bulk cable current under the bundle shield for the baseline configuration of the aircraft

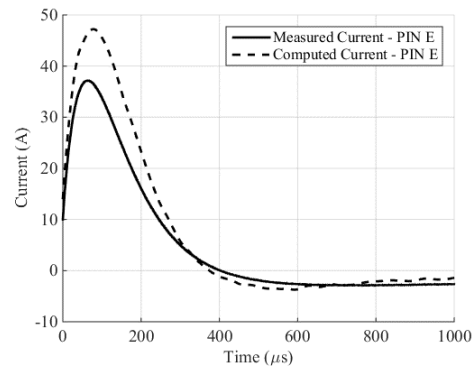


Fig. 13. Pin current on a 10 AWG wire on the baseline configuration of the aircraft

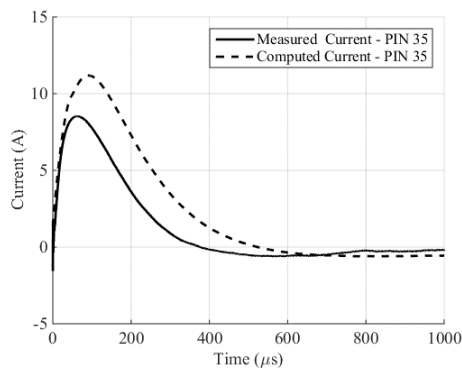


Fig. 14. Pin current on a 24 AWG twisted shielded pair on the baseline configuration of the aircraft

TABLE IV: SUMMARY OF RESULTS – SHORT CIRCUIT CURRENT IN AMPERE FOR BASELINE AIRCRAFT CONFIGURATION

	Cable Bundle	PIN 01	PIN 11	PIN 35	PIN E
Measurement	243.0	8.0	10.0	11	37.0
Calculation	212.0	10.9	9.5	9.5	47.1

The effects of the design modification were computed considering the aircraft installation and are presented in

Table V, Fig. 13 and Fig. 14. By implementing this change, the coupled levels increased by 4.76 dB in the worst case. It is

worth noting though, that the related electronic equipment was designed and verified according to the RTCA DO-160G section 22.0 tests methods to withstand an even higher level with enough safety margins.

TABLE V: SUMMARY OF RESULTS – COMPUTED CURRENT IN AMPERE

	Cable Bundle	PIN 01	PIN 11	PIN 35	PIN E
Baseline	212.0	10.9	9.5	9.5	47.1
Modified	258.0	17.3	13.7	13.7	71.8

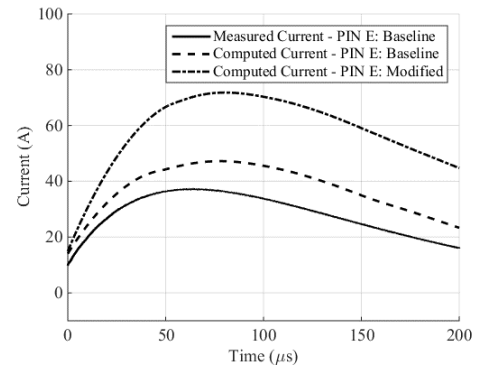


Fig. 15. Effect of the design change on the short circuit current through the power cable

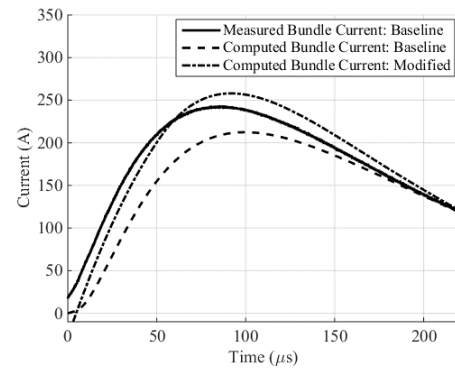


Fig. 16. Effect of the design change on the bulk cable current through the signal bundle

IV. CONCLUSIONS

In this study, low-level injection techniques and analytical methods were applied to determine the electromagnetic environment inside a metallic aircraft subjected to the direct attachment of a severe lightning strike. The results allowed a thorough understanding of the electromagnetic coupling to the interconnecting cables of an air data speed sensor and supported the understanding of the dominant physical mechanisms that allow the current transfer through the low-inductance / low-resistance paths in the actual aircraft installation. Furthermore, the validated numerical model was used to predict the coupling to a configuration that could not, be assessed during the full aircraft verification tests. The new control levels for equipment design were defined by applying appropriate scaling factors, derived from a combination of bench/aircraft low-level injection tests and numerical modeling.

REFERENCES

- [1] SAE ARP5412B, "Aircraft lightning environment and related test waveforms".
- [2] F.A. Fisher, J.A. Plumer, and R.A. Perala, "Lightning protection of aircraft". Lightning Technologies, 2004.
- [3] SAE ARP5415A, "User's manual for certification of aircraft electrical/electronic systems for indirect effects of lightning".
- [4] SAE ARP5416, "Aircraft lightning test methods".
- [5] I. A. Baratta, J. A. Mariano and C. B. Andrade, "Assessment of the FSV technique for shielding effectiveness and antenna coupling problems," in 2016 Proc. MOMAG Conf.
- [6] G. G. Gutiérrez, E. P. Gil, D. G. Gomez, and J. I. P. Gomez, "Finite-difference time-domain method applied to lightning simulation and aircraft certification process," in 10th International Symposium on Electromagnetic Compatibility, York, 2011, pp. 750-755.
- [7] B. D. Sherman, T. He, B. Nozari and T. Rudolph, "MD-90 Transport aircraft lightning induced transient level evaluation by time domain three dimensional finite difference modeling," in 1995 International Aerospace and Ground Conference on Lightning and Static Electricity, Williamsburg, 1995, pp. 69-1 to 69-15.